Nonideality in the composition dependence of viscosity in binary mixtures

Goundla Srinivas, Arnab Mukherjee, and Biman Bagchi*
Solid State and Structural Chemistry Unit, Indian Institute of Science, Bangalore-12, India

In this work we introduce two models to understand the anomalous composition dependence of viscosity of binary mixtures. Both models consist of a mixture of two molecular species (*A* and *B*) with the same diameter and mass but varying solute–solvent Lennard-Jones interaction. In model I, the two different species are strongly attractive while in model II, the attraction is weaker than that between the pure components. We have carried out extensive computer simulations of the two models. In addition, we study mode coupling theory for the viscosity of binary mixtures. *Both* the molecular dynamics simulations and the microscopic theory show the emergence of *strong* nonideality even in such simple systems. Model I shows a positive departure from ideality while model II shows the reverse behavior. The reason can be traced to the enhanced mean square stress fluctuations (MSSF) in the model I but decreased MSSF in the model II. The models show deviations (from ideality) very similar to the ones observed in experiments.

I. INTRODUCTION

Binary mixtures are well known to show a marked departure from the ideal behavior given by the Raoult's law.[1–4] For a given property P, the latter predicts the following simple dependence on the composition

$$P = x_1 P_1 + x_2 P_2, \tag{1}$$

where x_i's are the mole fractions and P_i's are the values of the property P of the pure (single component) liquids. More often than not, significant deviation from Eq. (1) is observed which is usually denoted by an excess function

$$P_{ex} = P - (x_1 P_1 + x_2 P_2). \tag{2}$$

Considerable literature exists on such behavior, where P can be volume, free energy, or viscosity. The last quantity is the topic of the present work.

The deviation from ideality appears to have a correlation with the solute–solvent mutual interaction. Despite the importance and the long interest in this problem, there does not seem to exist a satisfactory explanation of this nonideality (or nonadditivity) in binary mixtures. In fact, we are not aware of any microscopic study (based on the time correlation function approach) of the anomalous (or nonmonotonous) composition dependence of viscosity. This is, however, not surprising because a microscopic calculation of viscosity is quite difficult. In the absence of any microscopic theory, the experimental results have often been fitted to several empirical forms. Prominent among them is Eyring's theory of viscosity[4] extended to treat binary mixtures. This theory can correlate (with the help of one adjustable parameter) several aspects of the composition dependence of viscosity of many liquid mixtures (like benzene+methanol, toluene+methanol, etc.).[5] However, the very basis of Eyring's theory has been questioned, as this theory is based on the creation of holes of the size of the molecules, which is energetically unfavorable.

There also exist several other empirical expressions which attempt to explain this anomalous dependence of viscosity in binary mixtures.[6] On the experimental side there are evidences of the correlation between excess viscosity and excess volume of the liquid mixture where it has been observed for many cases that if excess volume is positive then excess viscosity becomes negative and vice versa.[2,3]

In recent years several interesting theoretical and computer simulation studies on Lennard-Jones (LJ) binary mixtures have been carried out.[7–9] These studies have concentrated mainly on the glass transition in binary mixtures which are known to be good glass formers (in contrast to the one component LJ liquid which does not form computer glass easily). In addition, these studies have considered only one particular composition and a unique interaction strength.[7–9] Considerable research has also been carried out by using the equilibrium molecular dynamic simulation method to determine the transport properties such as self[10–12] and mutual diffusion coefficients[13,14] in binary mixtures. Nonequilibrium molecular dynamic (MD) simulation methods have also been employed to determine the shear viscosity and thermal conductivity of binary soft-sphere mixtures.[15,16] Heyes carried out the extensive equilibrium MD simulations of Lennard-Jones binary mixtures by using both the microcanonical ($N\ V\ E$) and canonical ($N\ V\ T$) ensemble methods to study the partial properties of mixing and transport coefficients by adopting the time correlation function approach.[17] Apart from the bulk viscosity, these simulations seem to have satisfactorily reproduced the experimentally determined transport coefficients for the Ar–Kr mixture.[18]

However, the strong nonideality in the composition dependence of viscosity, observed in many experiments, has not been addressed to in the work of Heyes[17] or by others. The nonideality in the case of inert gas mixtures is small,

*Electronic mail: bbagchi@sscu.iisc.ernet.in

since their mutual interaction strength ($\in_{AB}$) follows the Berthelot mixing rule. To capture this strong nonideality we introduce and study two models (referred to as model I and model II) of binary mixtures in which the solute–solvent interaction strength is varied by keeping *all the other parameters* unchanged. All the three interactions (solute–solute, solvent–solvent, and solute–solvent) are described by the Lennard-Jones potential. Among the two models, one (model I) promotes the structure formation between solute and solvent molecules due to strong solute–solvent attractive interaction. The second model (model II) leads to the opposite scenario by promoting the structure breaking, because of weak solute–solvent interaction. These two models are perhaps the simplest models to mimic the structure making and structure breaking in binary mixtures. For convenience, we denote the solvent molecules as *A*, and the solute molecules as *B*. Note that *A* and *B* have the same radius and the same mass.

In the work reported here, extensive MD simulations and detailed mode coupling theory (MCT) calculations of the composition dependence of viscosity have been carried out for both models I and II. Model I shows a pronounced *positive* deviation from ideality at the intermediate composition, precisely of the type observed in many experimental situations. Further analysis shows that this nonideality is driven by the enhancement in the value of the mean square stress fluctuation. We found that a simple mode coupling theory provides a good agreement of the qualitative features. Model II shows a *negative* deviation from ideality—the signature of the structure breaking—leading to an enhancement of fluidity and lowering of viscosity. The agreement between computer simulation and the mode coupling theory calculations suggest that one can indeed propose a quantitative explanation of the nonideality in the composition dependence of viscosity in terms of interaction among and between the two species.

One should note that any microscopic calculation of viscosity (or any transport property) of a binary mixture has to deal with a broad phase separation region when the two species ''dislike'' each other. In this limit, one is restricted to high temperatures.

Organization of the rest of the article is as follows. In the next section we describe the basic definitions and the main equations that have been used in the present mode coupling theory. In Sec. III, we present the simulation details and the models used in this study. Detailed description of the microscopic theory is given in Sec. IV. Section V contains the results and discussion. We close the article with a few conclusions in Sec. VI.

II. BASIC DEFINITIONS

Microscopic expression for the time-dependent shear viscosity is formulated in terms of stress autocorrelation function and is given by

$$\eta(t)=(Vk_BT)^{-1}\langle\sigma^{xz}(0)\sigma^{xz}(t)\rangle, \tag{3}$$

where σ^{xz} is the off-diagonal element of the stress tensor, defined as

$$\sigma^{xz}=\sum_{j=1}^{N}[(p_j^x p_j^z/m)+F_j^z x_j], \tag{4}$$

where F_j^z is the z component of the force acting on the jth particle and the corresponding position is x_j, p_j^z is the z component of the momentum of jth particle, m being the mass of the particle. To map the stress tensor for the binary mixture, the total number of particles N is divided into N_1 (number of solvent particles) and N_2 (number of solute particles) such that, $N_1+N_2=N$. Thus, σ^{xz} can be written as

$$\sigma^{xz}=\sum_{j=1}^{N_1}[(p_j^x p_j^z/m)+F_j^z x_j] + \sum_{j=N_1+1}^{N}[(p_j^x p_j^z/m)+F_j^z x_j]. \tag{5}$$

Note that the solvent particles are labeled from 1 to N_1 and solute particles from (N_1+1) to N. High frequency shear modulus is given by

$$G_\infty=(Vk_BT)^{-1}\langle(\sigma^{xz}(0))^2\rangle. \tag{6}$$

Finally, the frequency dependent viscosity is obtained by Laplace transforming $\eta(t)$,

$$\eta(z)=\int_0^\infty dt\,\exp(-zt)\,\eta(t). \tag{7}$$

Experimentally observed viscosity is given by the zero frequency limit of $\eta(z)$.

III. SIMULATION DETAILS

We have carried out a series of molecular dynamic simulations of binary mixture by varying the solute mole fraction from 0 to 1. Our model binary system consists of a total of 500 [solvent(A)+solute(B)] particles. We have dealt with the microcanonical ensemble (constant N V E), by applying the usual periodic boundary conditions. Interaction between any two particles is given by the Lennard-Jones 12–6 potential

$$U_{ij}=4\epsilon_{ij}\left[\left(\frac{\sigma}{r_{ij}}\right)^{12}-\left(\frac{\sigma}{r_{ij}}\right)^{6}\right], \tag{8}$$

where i and j represent any two different particles. We set the diameter (σ) and mass (m) of both the solute and the solvent to unity, for simplicity. The solvent–solute interaction strength lies in the potential well depth ϵ_{AB}, where *A* and *B* represents the solvent and solute particles, respectively. Throughout this study we keep the interaction strength $\epsilon_{AA}=1.0$, (solvent–solvent), $\epsilon_{BB}=0.5$ (solute–solute). To account for the two models introduced in this study, we have dealt with the two very different solvent–solute interaction strength values, namely $\epsilon_{AB}=2.0$ in model I and $\epsilon_{AB}=0.3$ in model II. While the former accounts for the situation in which the solute and solvent attract each other stronger than they do their species, the latter describes the opposite scenario. In other words, the models in which $\epsilon_{AB}=2.0$ and $\epsilon_{AB}=0.3$ refer to the *attractive* and *repulsive* situations, respectively.

We set the reduced temperature $T^*(=k_BT/\epsilon)$ equal to unity in model I and 1.24 in model II. The reduced density $(\rho^*=\rho\sigma^3)$ is 0.85 in both the models. After many trial runs to verify the existing results on viscosity[19] of one component liquids, we have selected a time step $\Delta t^*=0.002\tau$ for model I, and $\Delta t^*=0.001\tau$ for model II for the integration of Newtonian equations of motion. The scaled time has been denoted as $\tau=\sigma\sqrt{m/\epsilon}$. We have dealt with six different solute compositions, namely 0.0, 0.2, 0.4, 0.6, 0.8, and 1.0. For each solute composition we have equilibrated the system up to 1.5×10^5 steps. Simulations carried out for another 2×10^5 steps after the equilibration during which the stress tensor has been calculated. We have also calculated the partial radial distribution functions in each case to make sure that the clustering or phase separation is avoided.

IV. FORMULATION OF THE MODE COUPLING THEORY

Any formulation of the MCT starts by separating the fast, short time decay from the slow, long time decay of the relevant time correlation function (tcf). The short time decay is assumed to occur from a few body (mainly binary) interactions whereas the long time decay is assumed to occur from coupling of the tcf to the binary product of the slow collective modes. Thus, the expression for the viscosity can be decomposed into two parts and written as[20,21]

$$\eta(t)=\eta_{\text{short}}(t)+\eta_{\text{collective}}(t). \tag{9}$$

Thus, central to the mode coupling theory development of any time correlation function is this assumption of the separation of time scales between the fast initial decay and the slow long time decay. The robustness of a mode coupling theory calculation actually depends critically on the accurate evaluation of the short time part. Not only does the short time part (often called the ''bare'' term) often contributes about 50% to the value of the transport coefficient (here viscosity), but also determines the magnitude of the contribution of the long time part. In fact, a central ingredient of both the short and the long time contributions is the static correlation functions.

The short time contribution, often referred to as the binary term, is assumed to be given by a Gaussian function. The rational for this assumption comes from the observation that only the even powers of time (t) appear in the short time expansion of $\eta(t)$ and collective term contribution starts as t^4. So the t^2 term contribution to binary viscosity can be approximated as a Gaussian function and can be written as[20,21]

$$\eta^{\text{bin}}(t)=G_\infty\exp(-t^2/\tau_\eta^2), \tag{10}$$

where τ_η, appearing in the above expression, can be determined by the second derivative of $\eta(t)$. The calculation of G_∞ and τ_η shall be described in Sec. IV A. As shown later, even the t^2 term requires three particle static correlation function. For pure liquids, calculations of binary terms have been reported by Balucani*et al.*[22] and also by Bhattacharrya and Bagchi.[23] In one component system, binary and MCT terms contribute approximately equally to the total viscosity. This is true at normal temperature and density, away from phase separation or glass transition points.

Any calculation of the MC part of viscosity needs the construction of the binary product of slow variables. The natural choice in case of a one component system is three current terms (two transverse and one longitudinal) and the density variable. At high density the decay of the current modes is fast and the dominant contribution comes from the density mode.[22–25] Therefore, we neglect the contributions of the current modes to the mode coupling term and retain only the density mode contribution.

In the case of a binary mixture, the construction of binary products is a bit difficult. The natural choice of slow density variables is the two partial densities, ρ_1 and ρ_2. In this there is one ambiguity though. What really plays an important role in the mode coupling theory calculation is the *local* density. These partial densities can be changed by an exchange mechanism and therefore, may not be regarded as ''good''slow variables. However, this exchange should become slow at high densities. Another possible choice is to retain the total density $(\rho_1+\rho_2)$ as the slow variable and choose the composition (χ), where $\chi=\rho_1-\rho_2$, as the second slow variable. According to the demand of MCT, χ is made orthogonal to ρ. We denote the orthogonal form of χ as χ_{og}, thus

$$\chi_{\text{og}}=\chi-(\langle\chi\rho\rangle\rho/\langle\rho\rho\rangle). \tag{11}$$

The mode coupling contribution to viscosity can be written as

$$\eta_{\text{collective}}(t)=\eta_{\rho\rho}(t)+\eta_{\chi_{\text{og}}\chi_{\text{og}}}(t). \tag{12}$$

There are situations where χ_{og} can play an important, even dominant, role. This happens near the phase separation. However, in the high density limit that we have considered, particularly for the models studied, this composition term does not appear to be important as shown by our preliminary calculations.

In the present work, we have considered *both* approaches to the mode coupling theory and found that they provide comparable results in both the attractive (model I) and repulsive (model II) cases. We refer to the set of MCT calculation in which ρ_1 and ρ_2 are the slow variables as scheme I and scheme II for the set in which the total density (ρ) considered as the slow variable. Note that the total density term contains equilibrium and dynamic cross correlations between the two species, in addition to the pure term contributions.

A. The binary term

Here we describe the formulation of the binary term. In this direction the first step is the calculation of the stress autocorrelation function, that is the value of the infinite frequency shear modulus G_∞ given by Eq. (6). With the help of Eq. (5), Eq. (6) can be reduced to the following exact form:

$$G_\infty=(\rho_1+\rho_2)k_BT + \frac{2\pi}{15}\sum_{i,j=1}^{2}\rho_i\rho_j\int_0^\infty dr g_{ij}(r)\frac{d}{dr}\left[r^4\frac{dv_{ij}(r)}{dr}\right], \quad (13)$$

where $i,j=1$ indicate solvent particles and $i,j=2$ denote solute particles. Thus, ρ_1 is the number density for the solvent particles and ρ_2 denotes the same for the solute particles. $g_{ij}(r)$ is the partial radial distribution function of the particles labeled i and j. Note that v_{ij} includes three different interaction potentials present between the solute and the solvent particles. By using Eq. (10), the expression for τ_η can be written as

$$\tau_\eta=\sqrt{\frac{-2G_\infty}{\ddot{\eta}(t=0)}}. \quad (14)$$

In the liquid region, $\eta(t)$ is mostly dominated by its potential part. Thus, using Eqs. (3) and (5), the expression for time dependent viscosity can be reduced to the following form:

$$\eta(t)=(Vk_BT)^{-1}\left\langle\left(\sum_{j=1}^{N_1}F_j^z x_j+\sum_{j=N_1+1}^{N}F_j^z x_j\right) \times\left(\sum_{k=1}^{N_1}F_k^z(t)x_k(t)+\sum_{k=N_1+1}^{N}F_k^z(t)x_k(t)\right)\right\rangle. \quad (15)$$

The second derivative of the total short time $\eta(t)$ is separated into contributions from two, three, and four particle correlation terms by using the proper choices of atomic labels,[22,23]

$$\ddot{\eta}(0)=\ddot{\eta}^2(0)+\ddot{\eta}^3(0)+\ddot{\eta}^{(4)}(0). \quad (16)$$

In the above expression of viscosity, the contribution of the four particle correlation term $\ddot{\eta}^{(4)}(0)$ is exactly zero.[22] The final expressions of the remaining two terms, $\eta^{(2)}(0)$ and $\eta^{(3)}(0)$, are given as

$$\ddot{\eta}^{(2)}(0)=\frac{-2\pi}{15m}\sum_{i,j=1}^{2}\rho_i\rho_j\int_0^\infty dr r^2[r^2(v_{ij}'')^2+2rv_{ij}''v_{ij}' +7(v_{ij}')^2]g_{ij}(r), \quad (17)$$

$$\ddot{\eta}^{(3)}(0)=\frac{-8}{75m}\sum_{ij,k=1}^{2}\rho_i\rho_j\rho_k\int_0^\infty dq q^2 h_{jk}(q) \times[3T_1^{ij}(q)T_1^{ik}(q)+2T_2^{ij}(q)T_2^{ik}(q)], \quad (18)$$

where the subscripts $i,j,k=1$ denote the corresponding properties of solvent particles and $i,j,k=2$ denote the same for the solute particles. $h_{jk}(q)$ is the Fourier transform of the pair correlation function. The integrals $T_1^{ij}(q)$ and $T_2^{ij}(q)$ [appearing in Eq. (18)] are defined as

$$T_1^{ij}(q)=\int_0^\infty dr r^2 J_3(qr)[rv_{ij}''(r)-v_{ij}'(r)]g_{ij}(r), \quad (19)$$

$$T_2^{ij}(q)=\int_0^\infty dr r^2 J_1(qr)[rv_{ij}''(r)+4v_{ij}'(r)]g_{ij}(r), \quad (20)$$

where $J_1(qr)$ and $J_3(qr)$ are the spherical Bessel functions. $v_{ij}'=dv_{ij}(r)/dr$ and $v_{ij}''=d^2v_{ij}(r)/dr^2$.

B. The mode coupling term

The mode coupling contribution to viscosity can be evaluated by using the general approach initiated by Bosse *et al.*[24] and further developed by Gestzi.[25] In this approach one starts with the general time correlation function expression for the shear viscosity in terms of the transverse current. One starts with a Mori-type rephrasing of the Green–Kubo formula for the shear viscosity. Thus, the expression for the viscosity can be written as

$$\eta=\lim_{\epsilon\to 0}\lim_{q\to 0}\frac{m^2}{q^2V}\int_0^\infty dt(QLj^x(\mathbf{q})| \times\exp(iQLQT-\epsilon t)|QLj^x(\mathbf{q})). \quad (21)$$

In the above equation $\mathbf{q}$ has been considered to be aligned along Z direction. L is the Hermitian Liouville operator. $Q=1-P$, where P is the projection operator which projects on to the chosen dynamical variable A^α. A^α is the set of slow variables which consists of three current densities and two particle densities for both the components which constitute the binary mixture. A^1, A^2, and A^3 are the commonly used three current densities.[24] A^4 and A^5 are choosen as the slow variables for densities of two different particles and defined as

$$A^4=\rho_1(\mathbf{q})=\sum_{j=1}^{N_1}\exp(-\mathbf{iq}\cdot\mathbf{r}_j), \quad (22)$$

$$A^5=\rho_2(\mathbf{q})=\sum_{j=N_1+1}^{N}\exp(-\mathbf{iq}\cdot\mathbf{r}_j). \quad (23)$$

$\rho_i(\mathbf{q})$ is the number density of the ith species (A and B). Species A and B are not to be confused with the dynamical variables A^α and $B_{\mathbf{k}}^i(\mathbf{q})$ (introduced later). The final expression for the mode coupling part of viscosity can be obtained by following the method outlined in Refs. 24 and 25 and is given by:

$$\eta_{\rho_i\rho_j}=\frac{k_BT}{60\pi^2}\int_0^\infty dq q^4\frac{S_{ii}'(q)S_{jj}'(q)}{S_{ii}^2(q)S_{jj}^2(q)}\int_{\tau_\eta}^\infty dt F_{ij}^2(q,t). \quad (24)$$

Note that the lower limit of the time integration has been changed from zero to τ_η to take out all the contributions of the order t^2 as the collective contributions are expected to start as t^4. τ_η is the characteristic time for Gaussian decay appeared in the expression of binary viscosity in Eq. (10). In the above expressions, the dynamical input parameters are the partial intermediate scattering functions $F_{ij}(q,t)$. The expressions of these functions are given in detail in the Appendix.

The total mode coupling contribution to the viscosity is obtained by summing together all the $\eta_{\rho_i\rho_j}$ terms (scheme I),

$$\eta_{\rho\rho}=\sum_{i,j=1}^{2}\eta_{\rho_i\rho_j}. \quad (25)$$

As discussed earlier, an alternative MCT approach is to treat the total density $\rho=\rho_1+\rho_2$ as the slow variable

(scheme II). In this approach the mode coupling contribution of ρ to the viscosity can be shown to be given by the following expression:

$$\eta_{\rho\rho}=\frac{k_BT}{60\pi^2}\int_0^\infty dqq^4[S_T'(q)/S_T(q)]^2 \times\int_{\tau_\eta}^\infty dt[F_T(q,t)/S_T(q)]^2, \quad (26)$$

where the *total* intermediate scattering function $F_T(q,t)$ is expressed as the sum of the partial intermediate scattering functions $F_{ij}(q,t)$ weighted by their mole fractions

$$F_T(q,t)=\sum_{i,j=1}^{2}\sqrt{x_ix_j}F_{ij}(q,t) \quad (27)$$

and the total static structure factor is defined as

$$S_T(q)=\sum_{i,j=1}^{2}\sqrt{x_ix_j}S_{ij}(q). \quad (28)$$

First derivative of the total static structure factor $S_T(q)$ is given by

$$S_T'(q)=\frac{\partial}{\partial q}S_T(q)=\frac{\partial}{\partial q}\sum_{i,j=1}^{2}\sqrt{x_ix_j}S_{ij}(q). \quad (29)$$

Preliminary calculations have shown that the contribution of the composition fluctuation term is much smaller than the total density term. We have, therefore, neglected the composition term. In fact, most of the calculations reported here have been performed with scheme I. We found that the total density term alone gives results quite similar to the ones obtained with $\rho_1(\mathbf{q})$ and $\rho_2(\mathbf{q})$ as the slow variables. This aspect will be discussed later.

MCT calculation with binary mixture requires determination of partial intermediate scattering functions. For one component system at density–temperature conditions away from the glass transition, we found that the continued fraction representation (based on the short time expansion) is quite adequate for the calculation of viscosity and friction, as discussed many years ago by Sjogren and Sjolander.[21] For binary mixtures, however, such a continued fraction calculation turns out to be quite difficult, because the second derivative of $F_{12}(q,t)$ is zero and the sign of the fourth derivative is oscillatory. We have, therefore, used an alternative approach to obtain $F_{ij}(q,t)$. $F_{ij}(q,t)$ is calculated from the time dependent density functional theory.[26] Expressions for $F_{ij}(q,t)$ are presented in the Appendix. For neat liquids, Munakata and Igarishi developed a self-consistent scheme to calculate dynamical correlation functions and applied it to calculation of the incoherent scattering function.[27] Self-consistent calculation of partial intermediate scattering function in the case of binary mixtures is rather difficult. Therefore, we have used a zero frequency binary diffusion coefficient as an input parameter in $F_{ij}(q,t)$, obtained by using η^{bin} in the Stokes–Einstein law. Expressions of all the relative basic quantities, necessary for the calculation of $F_{ij}(q,t)$, are given in detail in the Appendix.

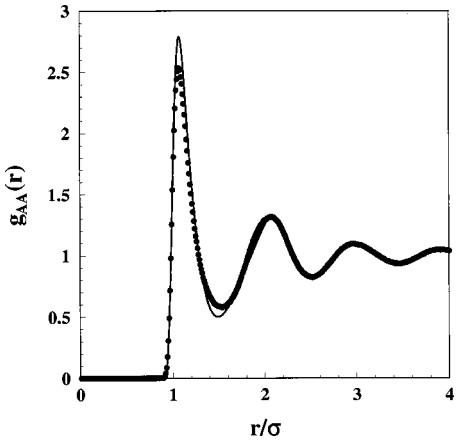

FIG. 1. The *solvent–solvent* partial radial distribution function $[g_{AA}(r)]$ obtained from MD simulations (represented by symbols) is compared with that obtained from the SMSA scheme (full line) for a 0.4 solute composition, for model I. Here $T^*=1.0$ and $\rho^*=0.85$.

V. RESULTS AND DISCUSSION

In Figs. 1 and 2, the solvent–solvent ($A-A$) and solvent–solute ($A-B$) partial radial distribution functions are plotted for model I ($\in_{AB}=2.0$) for 0.4 solute composition. In both figures the full line represents the theory and the symbols represent the simulation results. The theoretical lines are obtained by solving the Ornstein–Zernike equations for mixtures by using the soft mean spherical approximation (SMSA).[28] SMSA is known to provide a reasonably accurate description of radial distribution functions in dense liquids. For model I, both theory and simulations show a large first peak in $g_{AB}(r)$ (as shown in Fig. 2), compared to the respective one component neat liquids. For model II, we have observed the opposite effect—the first peak in $g_{AB}(r)$ is now reduced compared to neat liquids. While these are expected, the agreement between theory and simulation is by no means perfect. This is cause for some concern because we have used SMSA to obtain $g_{ij}(r)$ used in MCT calculations. How-

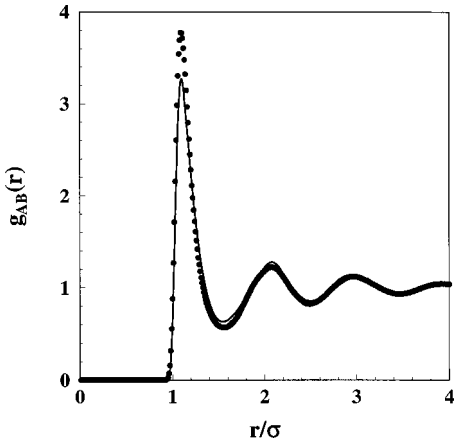

FIG. 2. The *solvent–solute* partial radial distribution function $[g_{AB}(r)]$ obtained from MD simulations is compared with that obtained from the SMSA scheme, for model I for the 0.4 solute composition. Full line represents the theory while the simulation result shown by symbols. T^* and ρ^* are the same as in Fig. 1.

ever, we find that despite this limitation, MCT can describe the basic features quite well. We shall come back to this point later.

As solute–solvent interaction strength affects the structure surrounding a solute/solvent to a great extent,[29,30] the above observed features in $g_{ij}(r)$ can be understood in terms of the solute–solvent interaction strength. While the enhanced attractive interaction between solute and solvent (model I) brings them closer together, the repulsive interaction forces the solute and solvent away from each other. In the former case as the solute–solvent interaction is favored over the relatively moderate solvent–solvent interaction and even weaker solute–solute interaction. The formation of solute–solvent nearest neighboring pair dominates. As a result the two adjacent shells of solute/solvent tend to be occupied by the opposite species. In other words, over a short distance, $A-B-A$ and $B-A-B$ repeating units shall be preferred. This feature is clearly reflected in the solvent–solute partial radial distribution function (Fig. 2). On the other hand, in the repulsive case (model II) solute and solvent molecules ''dislike'' each other. In this case, the solvent–solvent interaction is the strongest and the solute–solvent interaction is the weakest. Due to this hierarchy of interaction, the probability of finding the opposite species in the vicinity of a solute/solvent is very small. This explains the diminishing of first and second peaks in $g_{AB}(r)$ when the specific interaction is repulsive. In other words, the local structure around a solute/solvent is almost evacuated in terms of the opposite species.

In simulations, viscosity (η) is calculated by using the following expression:

$$\eta = \frac{1}{3k_B T^* V^*} \int_0^\infty \langle \sigma(0)\sigma(t)\rangle dt, \tag{30}$$

where V^* is the volume of the simulation box in reduced units and k_B is the Boltzmann constant. The remaining quantities appearing in the above expression are already described in the previous sections. Viscosity values obtained from simulation, as well as MCT, are plotted against the solute composition for the model I in Fig. 3 and for the model II in Fig. 4. In both the figures, simulation results are shown by symbols while the full line represents MCT prediction. Agreement between the theory and simulation is satisfactory for both the models over the entire composition range. The results presented in Figs. 3 and 4 are in qualitative agreement with the experimentally observed excess viscosity in binary mixtures.[5]

The stress autocorrelation functions (SACF) obtained from simulations are plotted in Figs. 5 and 6 against reduced time at various solute compositions, for models I and II, respectively. The respective stress auto correlation functions (without normalization) are plotted in the inset of each figure. Interestingly (as observed in both the models) the short time behavior of normalized SACF did not alter much either with the composition or with the specific interaction (as shown in main figures). We found that the major part of the observed difference in viscosity for these systems originates from the *zero time value of SACF*, which is the mean square stress fluctuation (MSSF). To make this point more clear, in

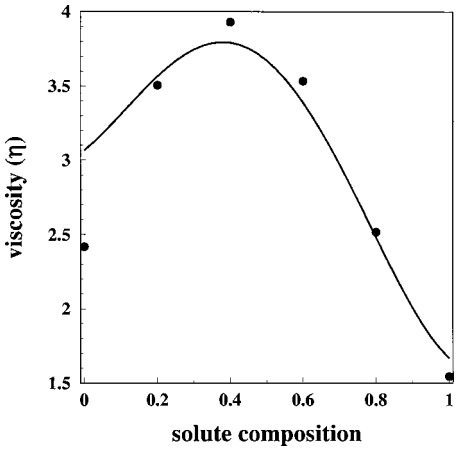

FIG. 3. The composition dependence of viscosity obtained from MD simulations is compared with the mode coupling theory predictions for model I. Symbols show the simulation results while the full line represents the MCT prediction. T^* and ρ^* are the same as in Fig. 1.

Fig. 7, we have plotted the high frequency shear modulus [given by Eq. (5)], obtained both from MD simulations and the microscopic method, for various solute compositions, for model I. Despite the differences in the magnitude, G_∞ obtained from the two different approaches (simulation and theory) shows similar behavior, over the entire composition range. The same is true for different interaction strengths. This is an important result which suggests that the significant contribution to the nonideal behavior of viscosity originates from the nonideality in the zero time stress correlation function.

As mentioned earlier, the viscosity values calculated according to the scheme II by using total density [$\rho(\mathbf{q})$] as the slow variable [with Eq. (26) as the MCT expression], agrees well with the ones obtained by using the scheme I. A comparison between the results obtained by using the two schemes are given in Fig. 8. Comparison between the two

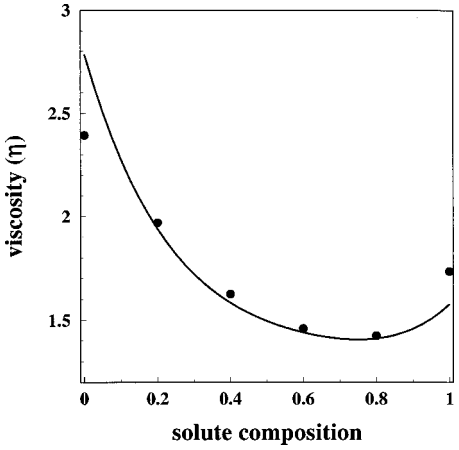

FIG. 4. The composition dependence of viscosity obtained from MD simulations is compared with the mode coupling theory predictions for model II. Symbols show the simulation results while the full line represents the MCT prediction. Here $T^*=1.24$ and $\rho^*=0.85$. This figure together with Fig. 3 shows that the agreement between the theory and simulation is good for most of the composition range for both the strong (model I) and weak (model II) solute–solvent interactions.

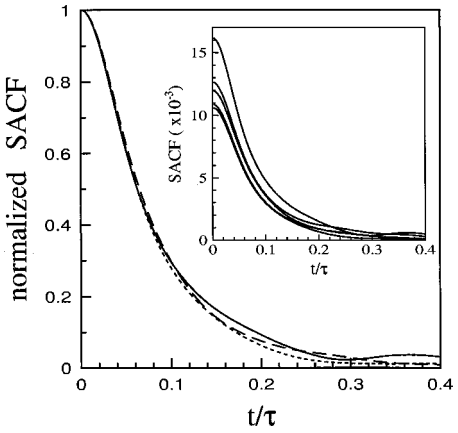

FIG. 5. The normalized stress auto correlation function obtained from MD simulations is plotted against the reduced time at various solute compositions for model I. Inset shows the same without normalization. For the sake of clarity, we have plotted only 0.0 (full line), 0.4 (large dashed line), and 0.6 (small dashed line) solute compositions in the main figure. In the inset, curves from top to bottom represent 0.0, 0.4, 0.6, 0.8, and 1.0 solute compositions. As shown in the main figure, short time behavior of normalized SACF remains unchanged with the composition. A large decrease in SACF is observed by increasing the solute composition (as shown in the inset). T^* and ρ^* are the same as in Fig. 1.

schemes for model I is shown in Fig. 8(a) while Fig. 8(b) shows that for the model II. The reason for this close proximity is that the partial intermediate scattering functions are not only small but also tend to cancel each other in the χ_{og} contribution.

As discussed earlier, the partial radial distribution functions obtained from SMSA are not in very good agreement with simulations. While this could be partly responsible for the lack of very good agreement between theory and simulation, the general features seem to be captured even by using SMSA.

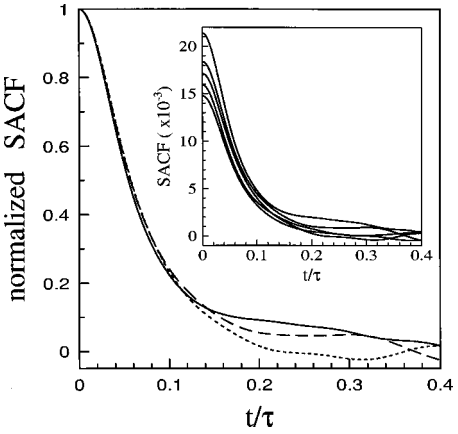

FIG. 6. The normalized stress auto correlation function obtained from MD simulations is plotted against the reduced time at various solute compositions for model II. The inset shows the same without normalization. Results for the solute compositions 0.0 (full line), 0.4 (large dashed line), and 0.6 (small dashed line) are shown in the main figure, while the inset shows the results for solute compositions 0.0, 0.4, 0.6, 0.8, and 1.0. Here $T^*=1.24$ and $\rho^*=0.85$. Figures 5 and 6, together depict that the short time behavior of normalized SACF remains unchanged both with the composition and the interaction strength.

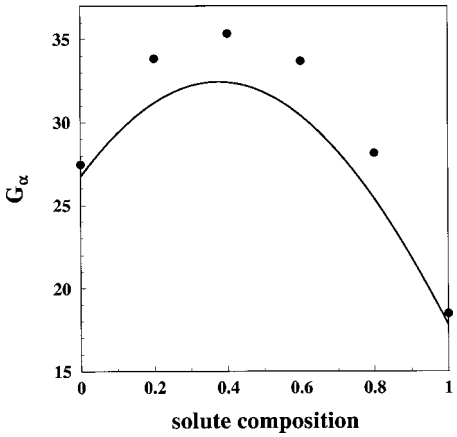

FIG. 7. High frequency shear moldulus values obtained from MCT and MD simulation are plotted against the solute composition for the model I. The full line shows the MCT result while the symbols represent that of the simulations. T^* and ρ^* are the same as in Fig. 1.

VI. CONCLUSION

In this article we have presented molecular dynamics simulations and mode coupling theory calculations of the composition dependence of viscosity of binary mixtures. We

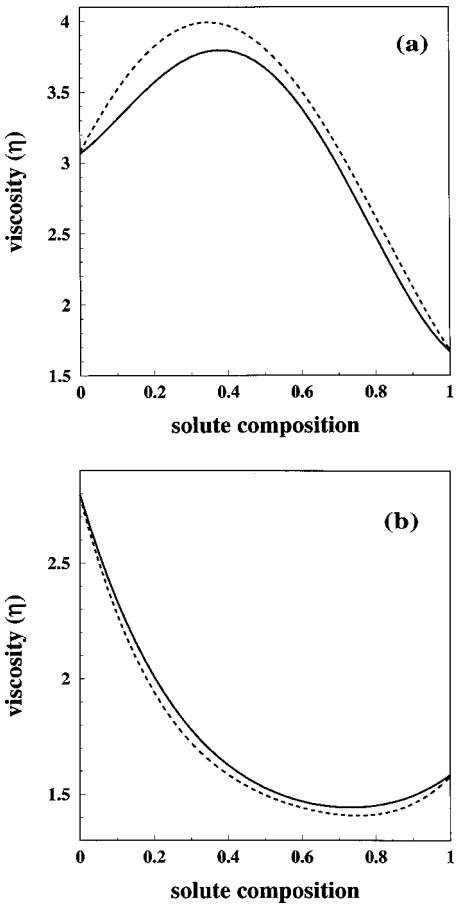

FIG. 8. The viscosities obtained from MCT by using two different mode coupling schemes are plotted as a function of solute composition. The full line shows the viscosity obtained by using scheme I while the result for scheme II is shown by the dashed line. (For the description of scheme I and scheme II, please see the text.) (a) represents the results for model I and (b) shows the same for model II.

have proposed two models to capture the essence of the wealth of experimental results that exist in the literature. In model I, the two components like each other more than they like themselves. In this case, we find nonideality in the positive direction. In model II, the two components dislike each other. This model is delicate because it often shows phase separation. We have studied this model at somewhat higher temperature. This model shows nonideality of the negative kind. In both cases agreement between theory and simulation is quite good, although not fully satisfactory. However, it is satisfying to note that both the theory and the simulations can capture the qualitative aspects of the composition dependence of viscosity.

The main reason for the anomalous composition dependence seems rather easy to understand. It arises from a similar dependence of the MSSF on the composition of the mixture. Thus, it is fair to say that the anomaly has a structural, rather than a dynamic, origin. The dynamics, of course, play an important role in augmenting the effect. The reason for the nonmonotonous composition dependence of MSSF arises from its dependence on the force acting on each molecule.

It is worth emphasizing that in both models the components have the same radius and the same mass. In addition to the emergence of significant nonideality, we found an important result that nonideality in both the models is driven by the zero time value of the shear stress autocorrelation function which is proportional to the infinite frequency shear bulk modulus G_∞. Dynamical correlation seems to follow the lead given by the static correlations, as is most often the case at normal liquid temperatures far above the glass transition temperature.

In this work we have not explored the composition dependence that can arise from the difference in sizes of *A* and *B*. Work in this direction is under progress.

We have already stressed that the MCT calculations presented here are not self-consistent. The reason for this is that an accurate short time description of the partial intermediate scattering function $F_{12}(q,t)$ is not available. Thus, we could not proceed via the usual route of constructing continued fraction representation of $F_{ij}(q,t)$ and then solve the mode coupling theory expression for friction consistently with the viscosity. Earlier experience has shown that nonself-consistent theories provide reasonably accurate estimate (within 10%–20%) of the zero frequency value of the friction and viscosity, so long one is far above the glass transition temperature, as is the case here.

The present study suggests many future problems. A more detailed study of the density and temperature dependence of nonideality is required. The present simulations have been carried out in the microcanonical ($N\ V\ E$) ensemble. We need to carry out similar simulations at constant pressure ($N\ P\ T$). The present calculations clearly show the need for more accurate description of the partial radial distribution function of binary mixtures. We need also to consider the case where the constituents have different radii. Work in these directions is under progress.

ACKNOWLEDGMENTS

It is a pleasure to thank Professor A. Yethiraj, Dr. K. Miyazaki, and Dr. Srikanth Sastry for the discussions on various aspects of this work. The authors are particularly indebted to Professor A. Yethiraj for providing them with the SMSA program. This work was supported in part by the Department of Science and Technology, India and CSIR, New Delhi, India. One author G. S. thanks CSIR for a research fellowship.

APPENDIX

Partial static structure factors are calculated according to the following formula by using SMSA closure:

$$S_{ij}(q)=\delta_{ij}+\sqrt{\rho_i\rho_j}h_{ij}(q). \tag{A1}$$

The intermediate scattering function is defined as the density auto correlation function as given as

$$F_{ij}(q,t)=(N_iN_j)^{-1/2}\langle\rho_i(\mathbf{q},t)\rho_j(-\mathbf{q},0)\rangle. \tag{A2}$$

We denote $F_{ij}(q,z)$ [Laplace transform of $F_{ij}(q,t)$] as the partial dynamic structure factor. Using time dependent density functional theory, the four coupled equations that are obtained for the dynamic structure factors are given as

$$F_{ij}(q,z)=[z+D_i(z)q^2]^{-1}S_{ij}(q)+\frac{D_i(z)q^2}{z+D_i(z)q^2}\times\sum_{k=1}^{2}\sqrt{\rho_i\rho_k}c_{ik}(q)F_{kj}(q,z). \tag{A3}$$

The four coupled equations ($i,j=1,2$) are solved to get the following expressions for partial dynamic structure factors:

$$F_{11}(q,z)=\frac{1}{Z(q,z)}[\{z+D_2^{\mathrm{bin}}(z=0)q^2(1-\rho_2c_{22}(q))\}\times S_{11}(q)+D_1^{\mathrm{bin}}(z=0)q^2\sqrt{\rho_1\rho_2}c_{12}(q)S_{21}(q)], \tag{A4}$$

$$F_{12}(q,z)=\frac{1}{Z(q,z)}[\{z+D_2^{\mathrm{bin}}(z=0)q^2(1-\rho_2c_{22}(q))\}\times S_{12}(q)+D_1^{\mathrm{bin}}(z=0)q^2\sqrt{\rho_1\rho_2}c_{12}(q)S_{22}(q)], \tag{A5}$$

$$F_{21}(q,z)=\frac{1}{Z(q,z)}[\{z+D_1^{\mathrm{bin}}(z=0)q^2(1-\rho_1c_{11}(q))\}\times S_{21}(q)+D_2^{\mathrm{bin}}(z=0)q^2\sqrt{\rho_1\rho_2}c_{21}(q)S_{11}(q)], \tag{A6}$$

$$F_{22}(q,z)=\frac{1}{Z(q,z)}[\{z+D_1^{\mathrm{bin}}(z=0)q^2(1-\rho_1c_{11}(q))\}\times S_{22}(q)+D_2^{\mathrm{bin}}(z=0)q^2\sqrt{\rho_1\rho_2}c_{21}(q)S_{12}(q)], \tag{A7}$$

and $Z(q,z)$ defined as

$$Z(q,z) = z^2 + z\Delta(q)[D_1^{\mathrm{bin}}(z=0)q^2 S_{22}(q) + D_2^{\mathrm{bin}}(z=0)q^2 S_{11}(q)] + D_1^{\mathrm{bin}}(z=0)D_2^{\mathrm{bin}}(z=0)q^4\Delta(q), \quad \text{(A8)}$$

where $\Delta(q)$ is defined as

$$\Delta(q) = [S_{11}(q)S_{22}(q) - S_{12}^2(q)]^{-1}. \quad \text{(A9)}$$

In the above expressions, all the frequency dependent diffusion coefficients are replaced by the respective binary diffusion coefficient values $D_1^{\mathrm{bin}}(z=0)$ and $D_2^{\mathrm{bin}}(z=0)$ which are obtained from Stokes–Einstein law at zero frequency by using only the binary part of the viscosity as follows:

$$D_1^{\mathrm{bin}}(z=0) = \frac{1}{2\pi\eta^{\mathrm{bin}}(z=0)\sigma_{11}}, \quad \text{(A10)}$$

$$D_2^{\mathrm{bin}}(z=0) = \frac{1}{2\pi\eta^{\mathrm{bin}}(z=0)\sigma_{22}}. \quad \text{(A11)}$$

[1] I. R. McDonald, Mol. Phys. **23**, 41 (1972).
[2] A. Pal and G. Daas, J. Mol. Liq. **84**, 327 (2000).
[3] R. S. Rama Devi, P. Venkatesu, and M. V. P. Rao, J. Chem. Eng. Data **41**, 479 (1996).
[4] S. Glasstone, K. J. Laidler, and H. Eyring, *Theory of Rate Processes* (McGraw-Hill, New York, 1941).
[5] L. Qunfang and H. Yu-Chun, Fluid Phase Equilibria **154**, 153 (1999).
[6] E. L. Heric, J. Chem. Eng. Data **11**, 66 (1966).
[7] W. Kob and H. C. Andersen, Phys. Rev. E **51**, 4626 (1995).
[8] W. Kob and H. C. Andersen, Phys. Rev. Lett. **73**, 1376 (1994).
[9] S. Sastry, Phys. Rev. Lett. **85**, 590 (2000).
[10] D. MacGowan, Mol. Phys. **59**, 1017 (1986).
[11] R. J. Bearman and D. L. Jolly, Mol. Phys. **51**, 447 (1984); **44**, 665 (1981).
[12] S. Toxvaerd, Mol. Phys. **56**, 1017 (1985).
[13] M. Schoen and C. Hoheisel, Mol. Phys. **52**, 33 (1984).
[14] O. F. Raineri and H. L. Friedman, Mol. Phys. **70**, 209 (1990).
[15] D. J. Evans and D. MacGowan, Phys. Rev. A **36**, 948 (1987); D. J. Evans and H. J. M. Hanley, *ibid.* **20**, 1648 (1979).
[16] S. Murad, D. P. S. Sethi, and P. V. Ravi, Fluid Phase Equilibria **53**, 159 (1989).
[17] D. M. Heyes, J. Chem. Phys. **96**, 2217 (1992).
[18] D. E. Diller, Physica A **104**, 417 (1980); D. E. Diller, Int. J. Thermophys. **3**, 237 (1982).
[19] D. M. Heyes, Phys. Rev. B **37**, 5677 (1988).
[20] U. Balucani and M. Zoppi, *Dynamics of the Liquid State* (Claredon, Oxford, 1994).
[21] L. Sjogren and A. Sjolandar, J. Phys. C: Solid State Phys. **12**, 4369 (1979).
[22] U. Balucani, R. Vellauri, and T. Gaskell, Phys. Rev. A **37**, 3386 (1988).
[23] S. Bhattacharyya and B. Bagchi, J. Chem. Phys. **109**, 7885 (1998); B. Bagchi and S. Bhattacharyya, Adv. Chem. Phys. **116**, 67 (2001).
[24] J. Bosse, W. Gotze, and M. Lucke, Phys. Rev. A **17**, 434 (1978).
[25] T. Geszti, J. Phys. C: Solid State Phys. **16**, 5805 (1983).
[26] A. Chandra and B. Bagchi, J. Chem. Phys. **112**, 1876 (2000).
[27] T. Munakata and A. Igarishi, Prog. Theor. Phys. **58**, 1345 (1977).
[28] W. G. Madden and S. A. Rice, J. Chem. Phys. **72**, 4208 (1980).
[29] G. Srinivas, S. Bhattacharyya, and B. Bagchi, J. Chem. Phys. **110**, 4477 (1999); R. Biswas, S. Bhattacharyya, and B. Bagchi, J. Phys. Chem. B **102**, 3552 (1998).
[30] R. M. Lynden-Bell and J. C. Rasaiah, J. Chem. Phys. **107**, 1981 (1997).